

## Supporting Information

for

### **Robust Synthesis of Green Fuels from Biomass-Derived Ethyl Esters Over Hierarchically Core/Shell-Structured ZSM-5@(Co/SiO<sub>2</sub>) Catalyst**

Darui Wang,<sup>ab</sup> Bo Wang,<sup>a</sup> Yu Ding,<sup>a</sup> Qingqing Yuan,<sup>a</sup> Haihong Wu,<sup>a</sup> Yejun Guan<sup>\*a</sup> and Peng Wu<sup>\*a</sup>

<sup>a</sup> Shanghai Key Laboratory of Green Chemistry and Chemical Processes, School of Chemistry and Molecular Engineering, East China Normal University, North Zhongshan Rd. 3663, Shanghai 200062, China

<sup>b</sup> State Key Laboratory of Green Chemical Engineering and Industrial Catalysis, Shanghai Research Institute of Petrochemical Technology, SINOPEC, Shanghai 201208, China.

#### **EXPERIMENTAL SECTION**

##### **Chemicals**

All chemicals and reagents were obtained from commercial suppliers and used without further purification: tetraethyl orthosilicate (Sigma-Aldrich,  $\geq 98\%$  Reagent Grade), tetrapropylammonium hydroxide (TCI, 25 wt% in water), colloidal silica (Sigma-Aldrich, 30 wt%), piperidine (Aladdin,  $\geq 99.5\%$  analytical standard), aluminum sulfate octadecahydrate (Aladdin, 98.0%–102.0% ACS reagent), sodium hydroxide (Alfa Aesar, 98.0% flake), ammonium chloride (Alfa Aesar,  $\geq 98\%$ ), aqueous ammonia solution (Sinopharm Chemical Reagent Co., Ltd., 28 wt%), ethanol (Sinopharm Chemical Reagent Co., Ltd.,  $\geq 99.7\%$  analytical standard),  $\text{Co}(\text{CH}_3\text{COO})_2 \cdot 4\text{H}_2\text{O}$  (Sinopharm Chemical Reagent Co., Ltd.,  $\geq 98\%$  analytical standard), ethyl levulinate (Sinopharm Chemical Reagent Co., Ltd.,  $\geq 99\%$  analytical standard), Air, H<sub>2</sub>, and N<sub>2</sub> gases (99.999 vol.%) were supplied by Shanghai Pujiang Specialty Gases Co., Ltd.

## Synthesis of ZSM-5 zeolite

ZSM-5 zeolites were synthesized with the assistance of active seeds. The active seeding gel was prepared according to the procedures reported previously.<sup>1</sup> Tetraethyl orthosilicate (TEOS) was dropped into the solution containing water and tetrapropylammonium hydroxide (TPAOH, 25% aqueous solution). After homogenizing at 80 °C for 2 h, the synthetic gel with a molar composition of 1.0 TEOS : 0.15 TPAOH : 14 H<sub>2</sub>O was introduced into a Teflon-lined steel autoclave and aged at 120 °C for 3 h. After cooling, the obtained seeding gel was directly used for the synthesis of ZSM-5 zeolites without any treatment.

ZSM-5 zeolite was synthesized from piperidine (PI) as structure directing agent, silica sol (30 wt% SiO<sub>2</sub>), aluminum sulfate and sodium hydroxide. Sodium hydroxide and aluminum sulfate were first dissolved in the aqueous solution of piperidine. Silica sol and active seeding gel were then dropped into the above solution and further stirred for 30 min, forming a gel composition of 1.0 SiO<sub>2</sub> : 0.0125 Al<sub>2</sub>O<sub>3</sub> : 0.2 PI : 0.05 Na<sub>2</sub>O : 25 H<sub>2</sub>O. SiO<sub>2</sub> in the active seeding gel accounted for 1% of the whole SiO<sub>2</sub> in gel. The gel was crystallized in a Teflon-lined steel autoclave at 170 °C for 72 h. The ZSM-5 product was collected by filtration followed by washing with distilled water several times, dried at 100 °C overnight, and then calcined in air at 550 °C for 6 h. The resulting ZSM-5 was brought into ammonium form *via* three consecutive exchanges in 1 M ammonium chloride solution at 80 °C for 2 h. After filtration, washing and drying overnight at 100 °C, the ammonium ion-exchanged zeolite was subsequently calcined at 550 °C for 6 h to give proton-type H-ZSM-5.

## Synthesis of ZSM-5@Co<sub>3</sub>(Si<sub>2</sub>O<sub>5</sub>)<sub>2</sub>(OH)<sub>2</sub>

ZSM-5@Co<sub>3</sub>(Si<sub>2</sub>O<sub>5</sub>)<sub>2</sub>(OH)<sub>2</sub> was prepared through a simple hydrothermal process. In a typical synthesis, Co(CH<sub>3</sub>COO)<sub>2</sub>·4H<sub>2</sub>O (0.127 g), NH<sub>4</sub>Cl (0.535 g) and NH<sub>3</sub>·H<sub>2</sub>O (0.91 g) were added under stirring in distilled water (50 g). As prepared H-ZSM-5 powder (0.1 - 0.3 g) was then added to the above solution and ultrasonicated for 30 min to form a uniform suspension, then the mixture was transferred to a Teflon autoclave (100 mL) and heated to 120 °C for 3 h. After the autoclave was cooled to room temperature, the resulting green precipitates were collected and washed

several times with distilled water and absolute ethanol. The final products were dried under vacuum at 60 °C for 4 h.

### **Synthesis of ZSM-5@(Co/SiO<sub>2</sub>)**

ZSM-5@Co<sub>3</sub>(Si<sub>2</sub>O<sub>5</sub>)<sub>2</sub>(OH)<sub>2</sub> was placed in a quartz boat in the middle of the horizontal tube furnace. After decomposition and reduction under a H<sub>2</sub> flow (flow rate: 100 mL min<sup>-1</sup>) at 550 °C for 4 h with a heating rate of 2 °C min<sup>-1</sup>, black powder of ZSM-5@Co was collected in the quartz boat at room temperature.

### **Synthesis of IM-Co/ZSM-5 by wetness impregnation method**

In a typical synthesis, Co(CH<sub>3</sub>COO)<sub>2</sub>·4H<sub>2</sub>O (1.27 g) was dissolved in distilled water (1 g), and then the solution was slowly dropped onto H-ZSM-5 (1 g) with continuous stirring at ambient temperature for 4 h. After completing this procedure, the material was firstly dried overnight at ambient temperature and then further at 110 °C for 12 h. Afterwards, the catalyst precursor was calcined in air (flow rate: 100 mL min<sup>-1</sup>) at 400 °C for 4 h and reduced under a H<sub>2</sub> flow (flow rate: 100 mL min<sup>-1</sup>) at 450 °C for 4 h with a heating rate of 2 °C min<sup>-1</sup>.

### **Catalytic reactions**

In a typical test, ethyl levulinate (2.5 mmol), ethanol (10 mL), and ZSM-5@(Co/SiO<sub>2</sub>) catalyst (0.1 g) were charged into a batch autoclave. The reactor was then flushed with N<sub>2</sub> for three times in order to remove the residual air, afterwards H<sub>2</sub> gas (3 MPa) was charged into the reactor when the temperature reached 250 °C. The reaction was conducted for 2 - 6 h at a stirring speed of 600 rpm. After reaction, the batch autoclave was cooled down quickly and the liquid products were analyzed by gas chromatography spectroscopy (Shimadzu 2014) equipped with a DB-FFAP capillary column (30 m × 0.25 mm × 0.25 μm).

For catalyst recycle, the catalysts were separated by centrifugation, washed with acetone to remove organics, dried in ambient air at 60 °C overnight. Without other treatments, the catalysts were reused in the next catalytic runs under the same conditions.

### **Characterization methods**

Powder X-ray diffraction (XRD) was employed to check the structure and crystallinity of the

zeolites. The XRD patterns were collected on a Rigaku Ultima IV diffractometer using Cu K $\alpha$  radiation at 35 kV and 25 mA in the 2 $\theta$  angle range of 5 - 80° using a step size of 0.02° and at a scanning speed of 10° min<sup>-1</sup>.

Nitrogen gas adsorption measurements were carried out at -196 °C on a BEL-MAX gas/vapor adsorption instrument. The samples were evacuated at 300 °C for at least 6 h before adsorption. The *t*-plot method was used to discriminate between micro- and mesoporosity. The surface areas were calculated by the Brunauer-Emmett-Teller (BET) method. The mesopore size distribution was obtained by the BJH model from the adsorption branches of the isotherms.

Acidity was measured by temperature-programmed desorption of ammonia (NH<sub>3</sub>-TPD) with a Micrometrics tp-5080 equipment equipped with a thermal conductivity detector (TCD) detector. Typically, 100 mg of sample was pretreated in helium stream (30 mL min<sup>-1</sup>) at 450 °C for 1 h. The adsorption of NH<sub>3</sub> was carried out at 50 °C for 1 h. The sample was flushed with helium at 100 °C for 2 h to remove physical absorbed NH<sub>3</sub> from the catalyst surface. The TPD profile was recorded at a heating rate of 10 °C min<sup>-1</sup> from 100 °C to 550 °C.

<sup>27</sup>Al solid-state MAS NMR spectra were recorded on a VARIAN VNMRS-400WB spectrometer under one pulse condition. The spectra were recorded at a frequency of 104.18 MHz, a spinning rate of 9.0 kHz, and a recycling delay of 4 s. KAl(SO<sub>4</sub>)<sub>2</sub>·12H<sub>2</sub>O was used as the reference for chemical shift.

Si, Co and Al contents were determined by inductively coupled plasma emission spectrometry (ICP) on a Thermo IRIS Intrepid II XSP atomic emission spectrometer.

The IR spectra were collected on a Nicolet Nexus 670 FT-IR spectrometer in absorbance mode at a spectral resolution of 2 cm<sup>-1</sup> using KBr technique (2 wt% wafer).

X-ray photoelectron spectra (XPS) were recorded on a Kratos AXIS UltraDLD X-ray photoelectron spectrometer at a pressure of about 2 × 10<sup>-9</sup> Pa with Al K $\alpha$  X-rays as the excitation source.

The pyridine-adsorption FI-IR spectra were also collected on a Nicolet Nexus 670 FT-IR spectrometer in absorbance mode at a spectral resolution of 2 cm<sup>-1</sup>. The sample was pressed into a

self-supported wafer with  $4.8 \text{ mg cm}^{-2}$  thickness, which was set in a quartz cell sealed with  $\text{CaF}_2$  windows and connected to a vacuum system. After evacuated at  $450 \text{ }^\circ\text{C}$  for 2 h, pyridine adsorption was carried out by exposing the pretreated wafer to a pyridine vapor at  $50 \text{ }^\circ\text{C}$  for 0.5 h. The adsorbed pyridine was evacuated successively at  $150 \text{ }^\circ\text{C}$  for 1 h. The spectra were collected at room temperature.

Scanning electron microscopy (SEM) was performed on a Hitachi S-4800 microscope to determine the crystal morphology.

Transmission electron microscopy (TEM) images were collected on a Tecnai G<sup>2</sup> F30 microscope. The sample was firstly made suspension in ethanol by ultrasonication, and a drop of such suspension was deposited onto a holey carbon foil supported on a copper grid. More than 300 particles were counted for the histograms of particle size distribution.

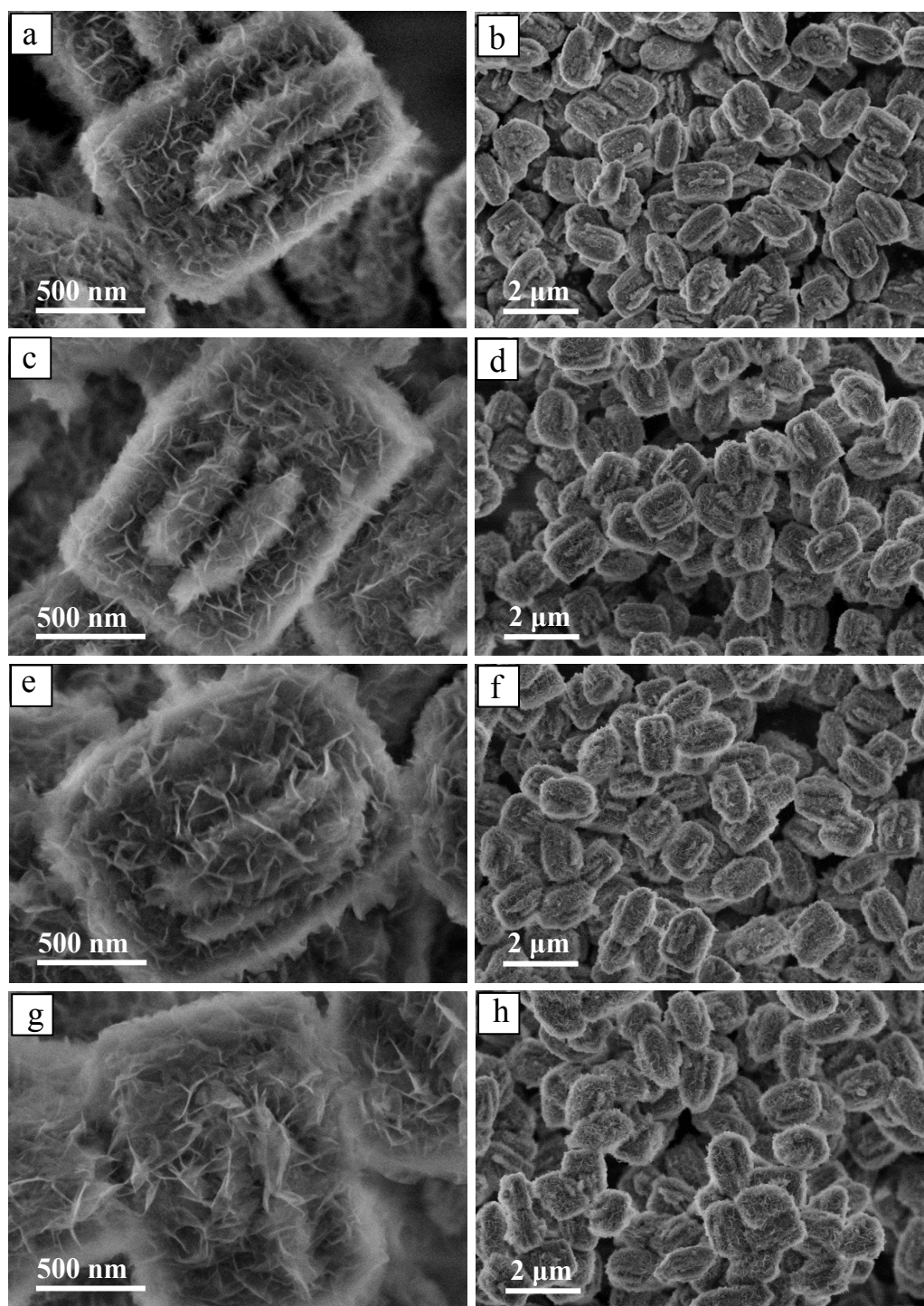


**Fig. S1** SEM images of ZSM-5@Co<sub>3</sub>(Si<sub>2</sub>O<sub>5</sub>)<sub>2</sub>(OH)<sub>2</sub> obtained at different temperature: 80 °C (a, b), 100 °C (c, d), 120 °C (e, f) and 140 °C (g, h).

*To investigate the effect of reaction temperature on the formation of hierarchical ZSM-5@Co<sub>3</sub>(Si<sub>2</sub>O<sub>5</sub>)<sub>2</sub>(OH)<sub>2</sub> composite materials, we monitored the reactions by changing the reaction temperature while fixing at 3 h. At lower temperatures of 80 °C and 100 °C, the flower-like*

*nanosheets were shorter, tighter and closely aggregated each other. At reaction temperature of 80 °C, only a small amount of flower-liked nanosheets were coated on the ZSM-5, and Co content was 7.8 wt% according to ICP analyses. At higher temperatures of 120 °C and 140 °C, the nanosheets exhibited a much clearer morphology, and became less aggregated. After reduction, the Co NPs supported on nanosheets are expected to aggregate more difficultly according to Ostwald ripening.<sup>2</sup> The Co content was leveled off at 120 °C, suggesting that the reaction was completed. The maximum loading of 10.1 wt% was close to the amount of Co source added. Therefore, we deem that well-structured ZSM-5@Co<sub>3</sub>(Si<sub>2</sub>O<sub>5</sub>)<sub>2</sub>(OH)<sub>2</sub> materials can be prepared by hydrothermal reaction at an optimal temperature of 120 °C for 3 h.*

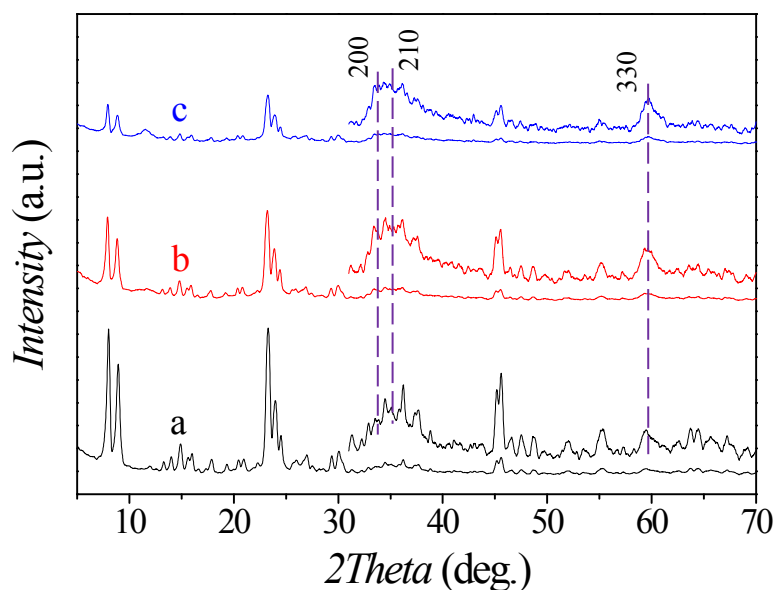


**Fig. S2** XRD patterns of ZSM-5@Co<sub>3</sub>(Si<sub>2</sub>O<sub>5</sub>)<sub>2</sub>(OH)<sub>2</sub> prepared with different Co loadings of 10.1 wt% (a), 20.2 wt% (b) and 30.0 wt% (c).

After the hydrothermal treatment in a Co<sup>2+</sup> containing solution, the resultant ZSM-5@Co<sub>3</sub>(Si<sub>2</sub>O<sub>5</sub>)<sub>2</sub>(OH)<sub>2</sub> showed additional XRD diffractions around 33.8°, 35.3° and 60.5° in the high angle region, which are indexed as the [200], [210] and [330] planes of cobalt silicate (Co<sub>3</sub>(Si<sub>2</sub>O<sub>5</sub>)<sub>2</sub>(OH)<sub>2</sub>, JCPDS No. 21-0871). The intensity of peaks indexed as Co<sub>3</sub>(Si<sub>2</sub>O<sub>5</sub>)<sub>2</sub>(OH)<sub>2</sub> increased when the Co contents increased from 10.1 to 30.0 wt%, while the intensity of peaks due MFI zeolite topology decreased.



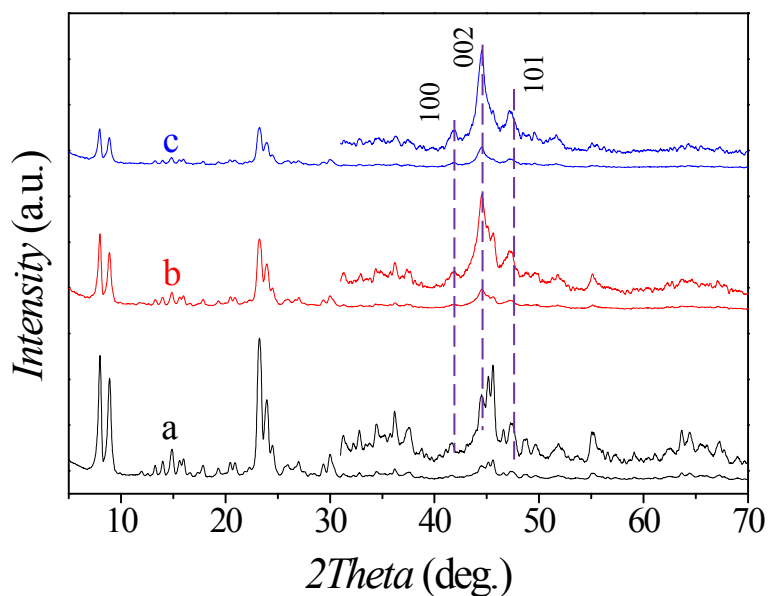


**Fig. S3** XRD patterns of ZSM-5@(Co/SiO<sub>2</sub>) prepared with different Co loadings of 10.1 wt% (a), 20.2 wt% (b) and 30.0 wt% (c).

After decomposition and reduction, the weak peaks centered at 41.7°, 44.8° and 47.6°, corresponding to the [100], [002] and [101] planes of Co metal (JCPDS No. 05-0727), were observed with the disappearance of the Co<sub>3</sub>(Si<sub>2</sub>O<sub>5</sub>)<sub>2</sub>(OH)<sub>2</sub>. Consistently, the intensity of peaks indexed as Co metal increased when the Co contents increased from 10.1 to 30.0 wt%, while the intensity of peaks due MFI zeolite topology decreased.

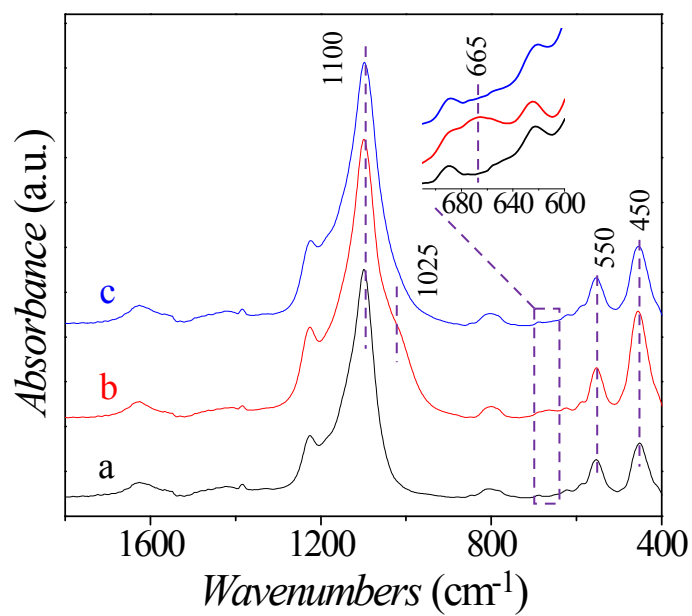


**Fig. S4** FT-IR spectra of the pristine ZSM-5 (a), ZSM-5@Co<sub>3</sub>(Si<sub>2</sub>O<sub>5</sub>)<sub>2</sub>(OH)<sub>2</sub> (b) and ZSM-5@(Co/SiO<sub>2</sub>) (c). The inset shows the enlarged region for Si-O-Co stretching vibration.

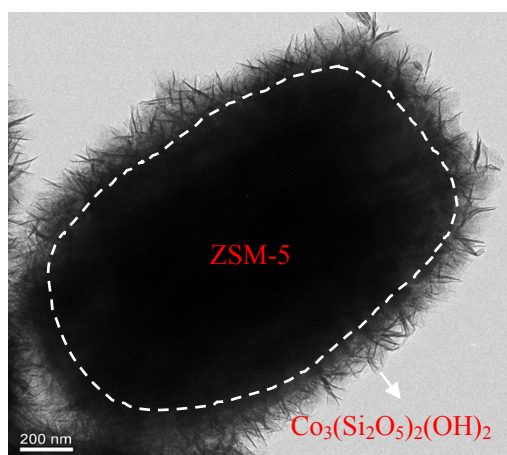


**Fig. S5** TEM image of ZSM-5@ $\text{Co}_3(\text{Si}_2\text{O}_5)_2(\text{OH})_2$ .

*The ZSM-5@ $\text{Co}_3(\text{Si}_2\text{O}_5)_2(\text{OH})_2$  precursors possessed a typical core/shell structure with flexible  $\text{Co}_3(\text{Si}_2\text{O}_5)_2(\text{OH})_2$  nanosheets uniformly coating on the ZSM-5 crystals. The TEM image clearly showed the junction between the shell and the core, in which the flower-like  $\text{Co}_3(\text{Si}_2\text{O}_5)_2(\text{OH})_2$  and the crystalline ZSM-5 crystal grew connectedly.*

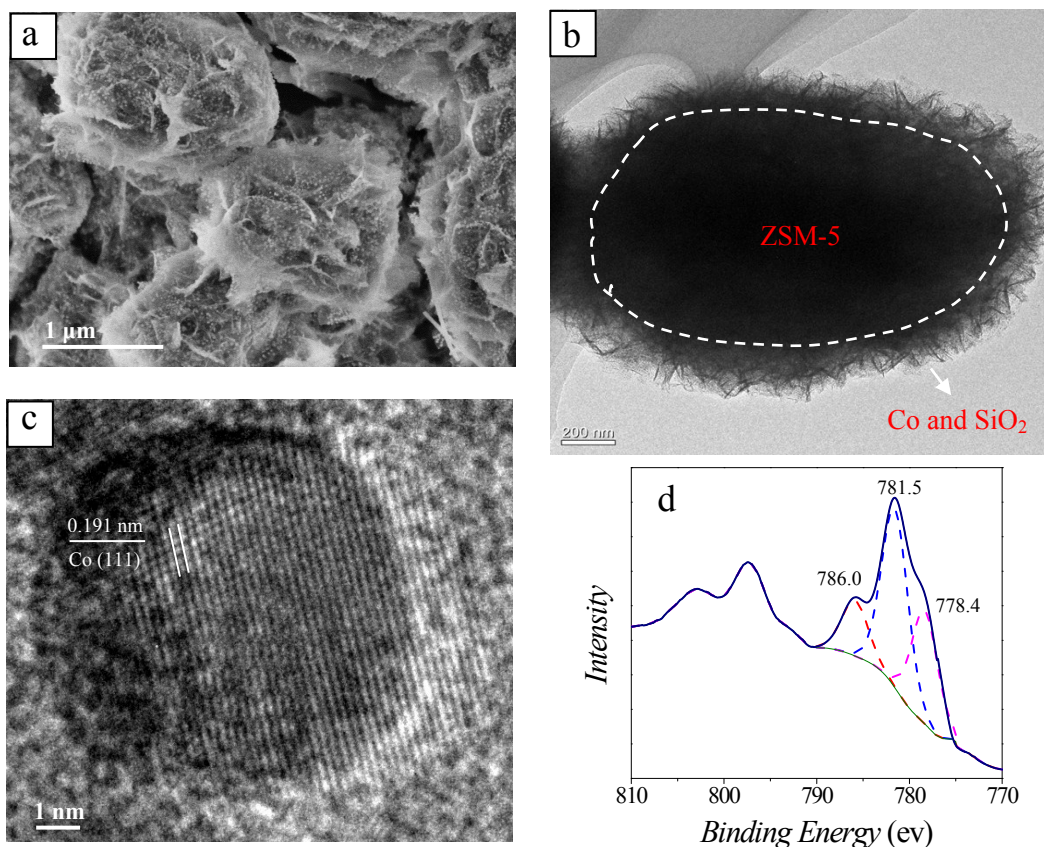


**Fig. S6** SEM image of ZSM-5@(Co/SiO<sub>2</sub>) (a), TEM images of ZSM-5@(Co/SiO<sub>2</sub>) (b) and metal Co (c), XPS spectrum of Co 2p of ZSM-5@(Co/SiO<sub>2</sub>) (d).

From the SEM and TEM images, we can see the core/shell structure was well maintained after decomposition and reduction and there were still flower-like nanosheets coating on the ZSM-5 crystals. Uniform Co nanoparticles were dispersed on the SiO<sub>2</sub> matrix, just like “diamond on the beach”. Co nanoparticles are expected to be more stable when located between two adjoining flower-like SiO<sub>2</sub> matrix, then sintering and leaching can be avoided during reaction at high temperature. This unique distribution pattern of metal nanoparticles are expected to lead to a high activity and stability during reaction. The distance of the adjacent lattice fringes in nanoparticles was determined to be about 0.191 nm, corresponding well to the  $d_{101}$  spacing of metal Co (JCPDS No. 05-0727). The chemical states of Co species were characterized by XPS technique, The Co 2p signal with a binding energy of 778.4 eV is assigned to metallic Co. In addition, the other two at 781.5 and 786.0 eV were also observed, which are attributed to unreduced cobalt silicate Co<sub>3</sub>(Si<sub>2</sub>O<sub>5</sub>)<sub>2</sub>(OH)<sub>2</sub>.

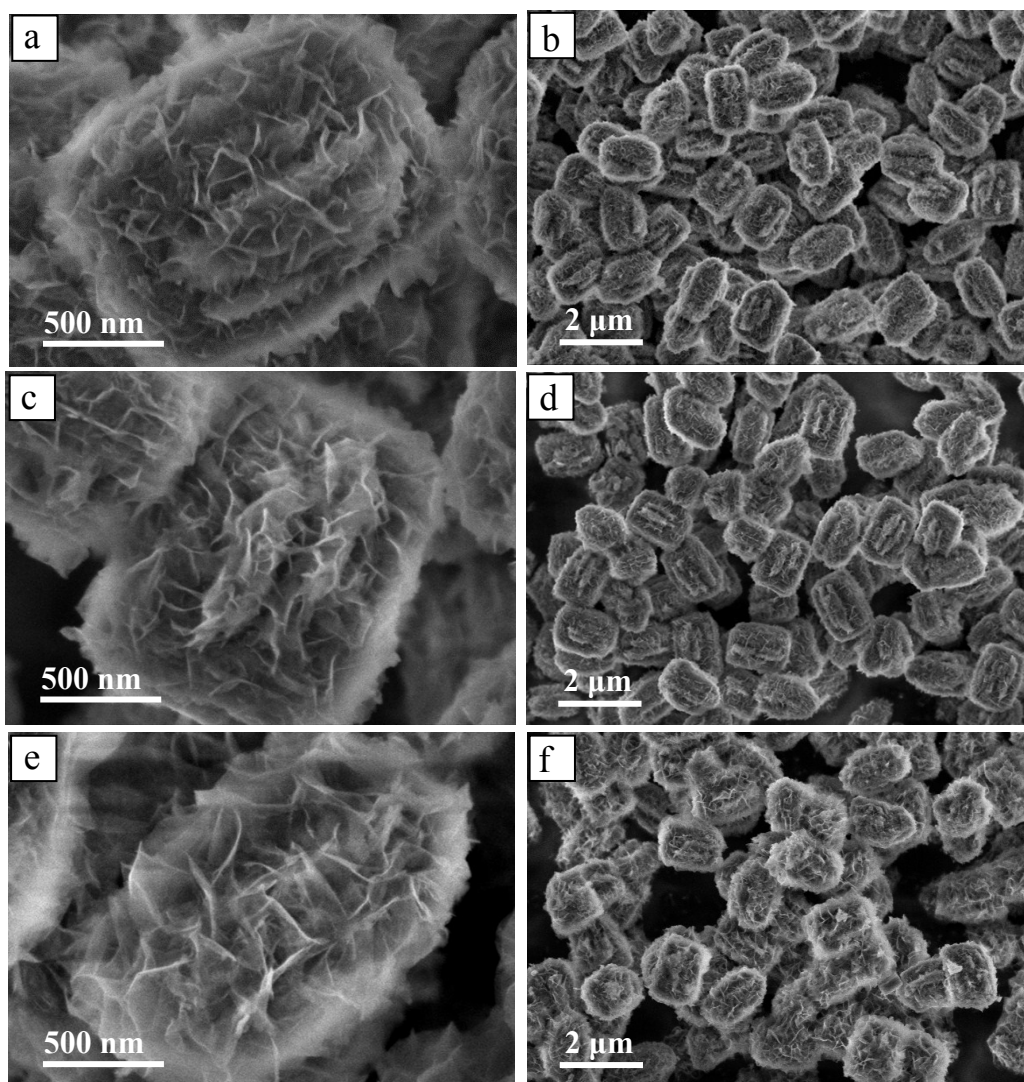


**Fig. S7** SEM images of ZSM-5@Co<sub>3</sub>(Si<sub>2</sub>O<sub>5</sub>)<sub>2</sub>(OH)<sub>2</sub> prepared with different Co loadings of 10.1 wt% (a, b), 20.2 wt% (c, d) and 30.0 wt% (e, f).

*The ZSM-5@Co<sub>3</sub>(Si<sub>2</sub>O<sub>5</sub>)<sub>2</sub>(OH)<sub>2</sub> composites always possessed core/shell structure when varying Co contents from 10.1 to 30.0 wt%. The above images showed that the amount of flowe-like Co<sub>3</sub>(Si<sub>2</sub>O<sub>5</sub>)<sub>2</sub>(OH)<sub>2</sub> nanosheets increased with an increasing Co content.*

**Table S1** The textural properties of the pristine ZSM-5, ZSM-5@(Co/SiO<sub>2</sub>) and IM-Co/ZSM-5 with different Co contents.

Catalyst	S <sub>BET</sub> <sup>a</sup> (m <sup>2</sup> g <sup>-1</sup> )	S <sub>ext</sub> <sup>b</sup> (m <sup>2</sup> g <sup>-1</sup> )	V <sub>tot</sub> <sup>c</sup> (cm <sup>3</sup> g <sup>-1</sup> )	V <sub>micro</sub> <sup>b</sup> (cm <sup>3</sup> g <sup>-1</sup> )	V <sub>meso</sub> <sup>d</sup> (cm <sup>3</sup> g <sup>-1</sup> )
Pristine ZSM-5	419	28	0.26	0.17	0.09
ZSM-5@(Co/SiO <sub>2</sub> ) (10.1 wt%) <sup>e</sup>	371	125	0.34	0.12	0.22
ZSM-5@(Co/SiO <sub>2</sub> ) (20.2 wt%)	367	155	0.39	0.10	0.29
ZSM-5@(Co/SiO <sub>2</sub> ) (30.0 wt%)	352	203	0.45	0.08	0.37
IM-Co/ZSM-5 (30.0 wt%)	320	17	0.19	0.11	0.07

<sup>a</sup> Obtained by BET method.

<sup>b</sup> Obtained by *t*-plot method.

<sup>c</sup> Given by the adsorption amount at P/P<sub>0</sub> = 0.99.

<sup>d</sup> V<sub>meso</sub> = V<sub>tot</sub> - V<sub>micro</sub>.

<sup>e</sup> The numbers in parentheses indicate the Co contents actually loaded as analyzed by ICP.

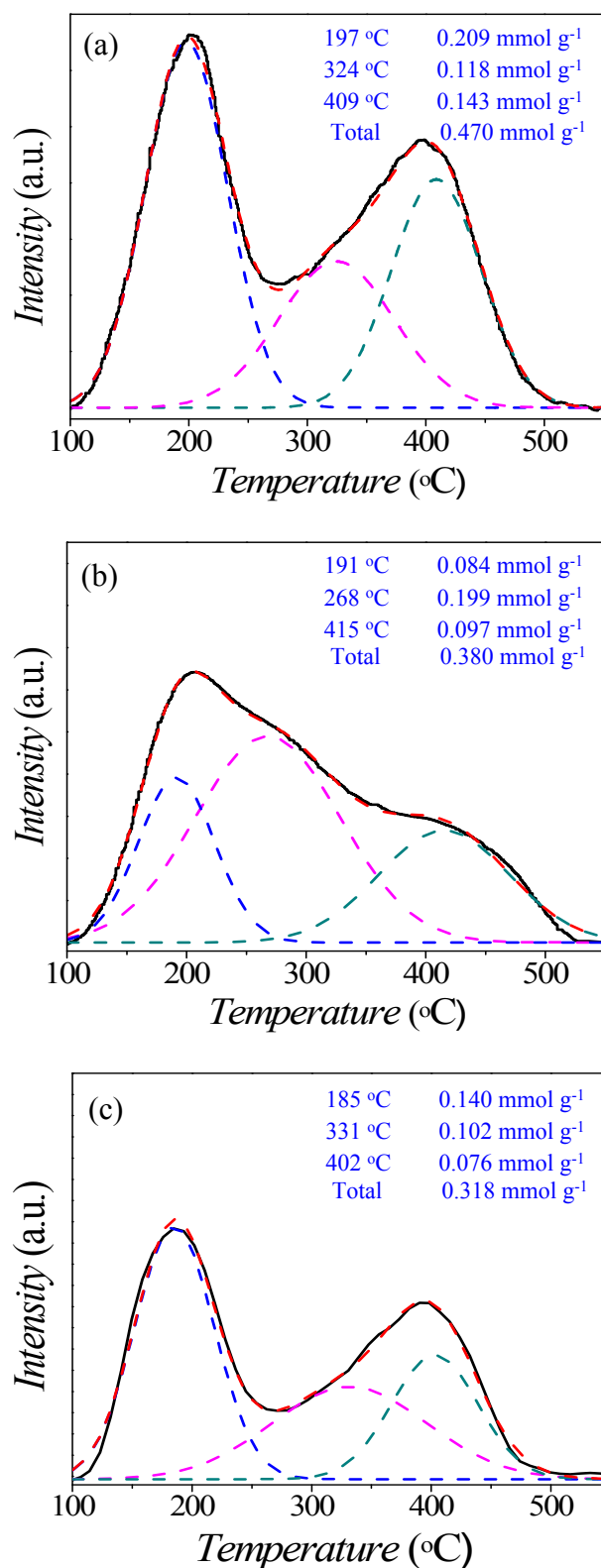


**Fig. S8** NH<sub>3</sub>-TPD profiles of pristine ZSM-5 (a), ZSM-5@(Co/SiO<sub>2</sub>) (b) and IM-ZSM-5/Co (c).

The Co contents were both ca. 30.0 wt% as given by ICP analyses.

Compared with pristine ZSM-5, ZSM-5@(Co/SiO<sub>2</sub>) possessed a slightly lower total acid quantity of 0.38 mmol g<sup>-1</sup>. And the strong acid quantity decreased from 0.143 mmol g<sup>-1</sup> to 0.097 mmol g<sup>-1</sup>, while the middle strong acid quantity increased from 0.118 mmol g<sup>-1</sup> to 0.199 mmol g<sup>-1</sup>, which may be due to the sacrifice of ZSM-5 crystals or a partial cation exchange between Co<sup>2+</sup> and H<sup>+</sup> during the hydrothermal reaction. IM-Co/ZSM-5 prepared by wetness impregnation method possessed the least total acid quantity of 0.318 mmol g<sup>-1</sup>. The weak acid quantity, middle strong acid quantity and strong acid quantity were 0.140 mmol g<sup>-1</sup>, 0.102 mmol g<sup>-1</sup> and 0.076 mmol g<sup>-1</sup>, respectively. Partial acid active sites may be covered by bulky Co nanoparticles. And atomic interaction between metal Co centers and protons also led to decrease in acidity strength of the Si(OH)Al groups in zeolites.<sup>3</sup> The SiO<sub>2</sub> matrices in the shell of ZSM-5@(Co/SiO<sub>2</sub>) served as binders between Co centers and protons, and atomic interaction can be efficiently weakened by SiO<sub>2</sub> matrices, strong acid quantity can be maintained at a high level.



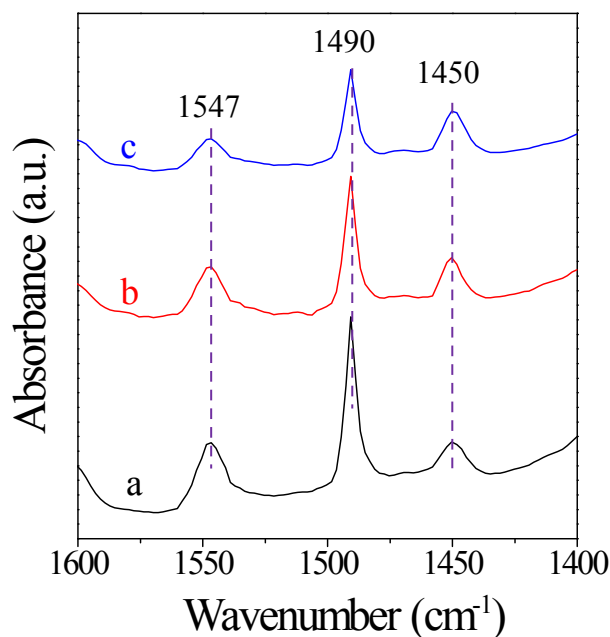


**Fig. S9** Pyridine-adsorption FT-IR spectra of pristine ZSM-5 (a), ZSM-5@(Co/SiO<sub>2</sub>) (b) and IM-Co/ZSM-5 (c). The Co contents were both ca. 30.0 wt% as given by ICP analyses.

The spectra were taken on proton-form samples after desorption of pyridine at 150 °C for 1 h. The stretching bands of at around 1547 and 1450 cm<sup>-1</sup> are attributed to Brønsted acid sites and Lewis acid sites, respectively.<sup>4</sup> Compared with pristine ZSM-5, the ZSM-5@(Co/SiO<sub>2</sub>) catalysts prepared by the novel method possessed slightly lower concentration of Brønsted acid sites, possible due to a partial sacrificing and dissolving of the crystalline structure of ZSM-5 during the hydrothermal reaction step. In addition, the concentration of Lewis acid sites increased after incorporating Co component. The unreduced inonic metal species were speculated to be potential Lewis acid sites, causing the increase in the Lewis acid concentration.<sup>5</sup> IM-Co/ZSM-5 possessed lowest concentration of Brønsted acid sites and similar concentration of Lewis acid sites as ZSM-5@(Co/SiO<sub>2</sub>). Brønsted acid sites may be weakened by atomic interaction between metal Co centers and protons or partial covered by bulky Co nanoparticles. The results were in good agreement with the conclusions from Fig. S8.

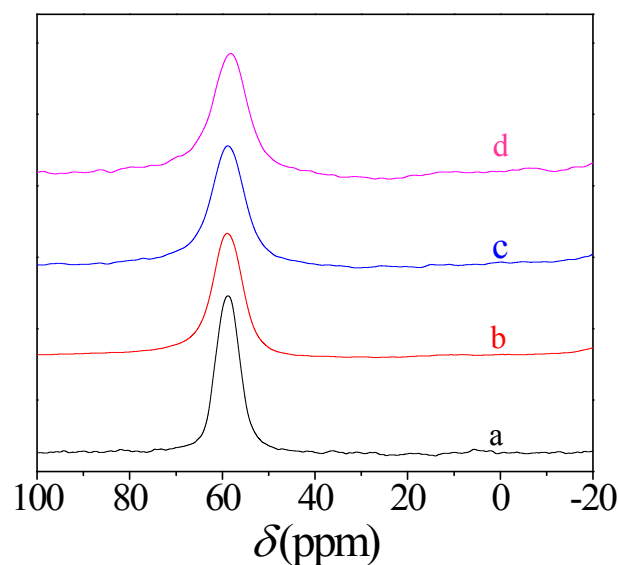


**Fig. S10**  $^{27}\text{Al}$  MAS NMR spectra of the pristine ZSM-5 (a) and ZSM-5@( $\text{Co}/\text{SiO}_2$ ) with cobalt loadings of 10.1 wt% (b), 20.2 wt% (c) and 30.0 wt% (d).

The  $^{27}\text{Al}$  MAS NMR spectra of the pristine ZSM-5 showed only one signal of tetrahedral Al at 58 ppm, but no resonance at 0 ppm due to octahedral Al, which means that the Al ions were incorporated predominantly in the framework position. After incorporating Co NPs, ZSM-5@( $\text{Co}/\text{SiO}_2$ ) also showed only one signal of tetrahedral Al at 58 ppm as pristine ZSM-5, but the signal became broader with the increased Co content. This implied that the microenvironment of Al became more asymmetric in coordination states. According to the ICP analyzes, the Si/Al molar ratios for the pristine ZSM-5 and ZSM-5@( $\text{Co}/\text{SiO}_2$ ) with a Co loading of 10.1, 20.2 and 30.0 wt% were 40.5, 41.2 and 40.6, respectively. According to the unchanged Si/Al ratios and above broadened signals, we can assume that Al was also extracted from ZSM-5 along with the silica dissolution and Al was incorporated into the cobalt silicate phase.

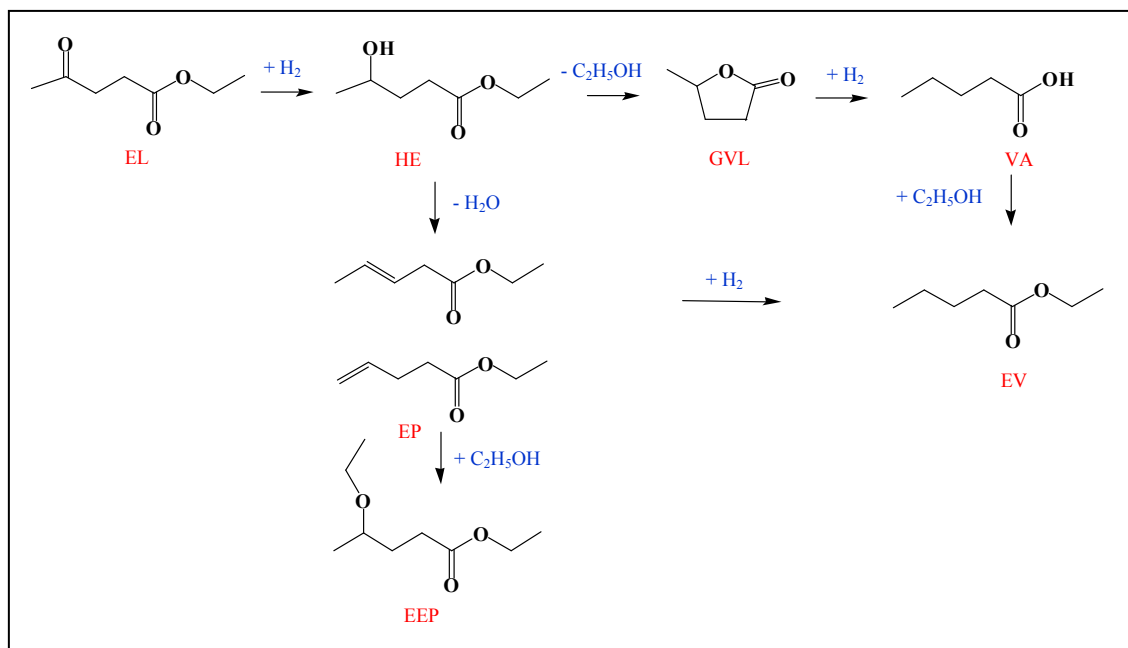


**Fig. S11** The reaction route of one-pot conversion of ethyl levulinate (EL) to ethyl valerate (EV) by ZSM-5@(Co/SiO<sub>2</sub>) in ethanol solution.

Firstly, the precursor ethyl levulinate (EL) undergoes hydrogenation to form 4-hydroxyethylvalerate (HE) on the active sites of metal Co NPs. Then HE was converted to  $\gamma$ -valerolactone (GVL) through dealcoholization, and GVL can be successfully ring-opened and hydrogenated to valeric acid (VA) by cooperation of acidic and metallic active sites. Further esterification of VA on acidic sites leads to the formation of desired product of ethyl valerate (EV). Meanwhile, HE can also be converted to by-product of ethyl pentenoate (EP) on acidic sites through dehydration. And EP is further converted to ethyl 4-ethoxy pentanoate (EEP) with an ethanol molecule by addition reaction.

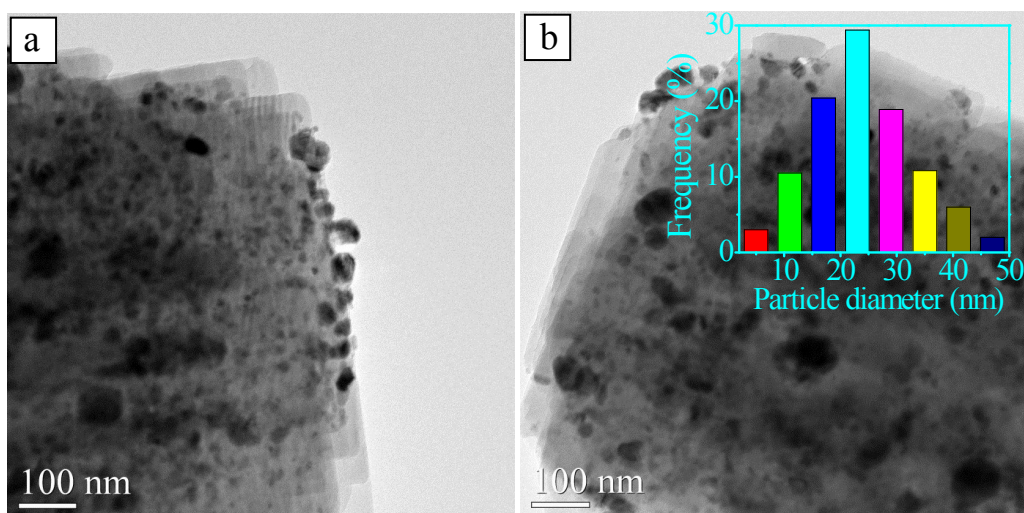


**Fig. S12** TEM image of IM-Co/ZSM-5 (30.0 wt% Co loading) prepared by wet impregnation method. Inset was the corresponding size distribution histogram of the Co nanoparticles.

*Compared with ZSM-5@(Co/SiO<sub>2</sub>), IM-Co/ZSM-5 prepared by wet impregnation method possessed larger Co NPs with diameters of 20 - 30 nm and no nanosheets were observed on the surface of ZSM-5 zeolite.*

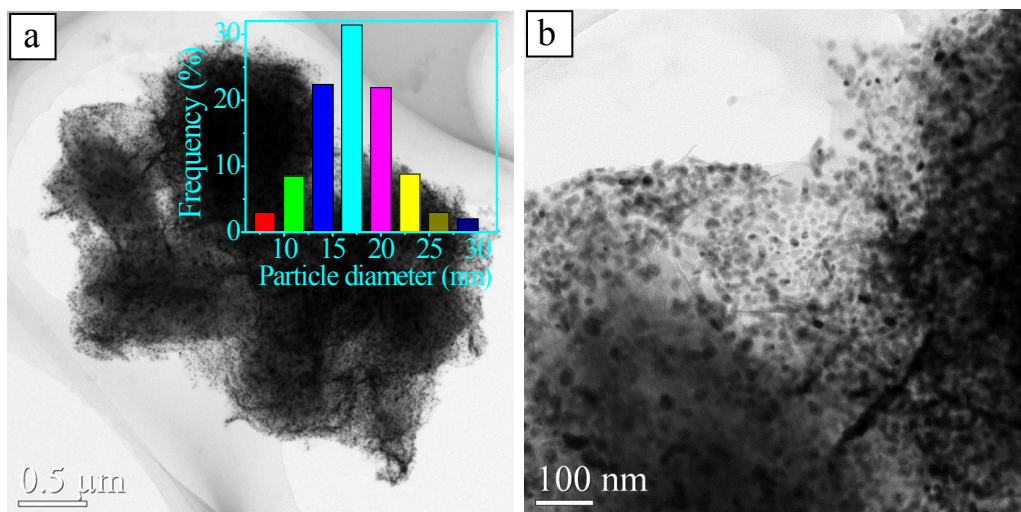


**Fig. S13** TEM images of ZSM-5@(Co/SiO<sub>2</sub>) (a, b) after four recycling runs. The inset was the corresponding size distribution histogram of the Co nanoparticles.

*From the TEM images, we can see the morphology of the nanosheets on ZSM-5 did not change during the reaction. As shown in inset image, the average diameters of Co particles were still much smaller (12 - 18 nm), more importantly, these particles were more evenly distributed with a deviation of 3.0 nm. According to ICP analyze, the Co content was 23.9 wt% for IM-Co/ZSM-5 after four recycling runs.*

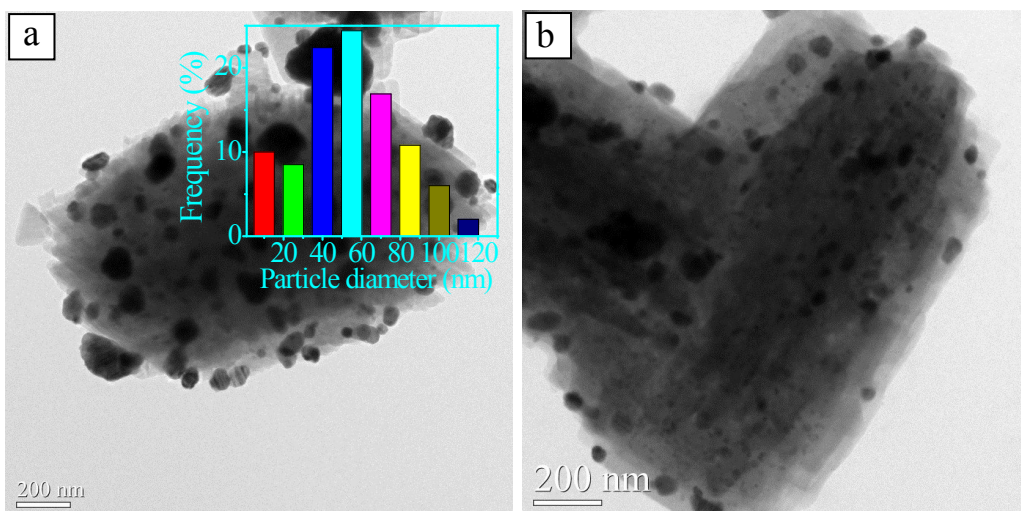


**Fig. S14** TEM images of IM-Co/ZSM-5 (a, b) after four recycling runs. The inset was the corresponding size distribution histogram of the Co nanoparticles.

*The much larger Co particles in impregnated catalysts were further aggregated during the catalytic reaction, a large portion (about 20%) of strongly aggregated Co particles (larger than 100 nm) was observed to coexist. According to ICP analyze, the Co content was 15.6 wt% for IM-Co/ZSM-5 after four recycling runs.*

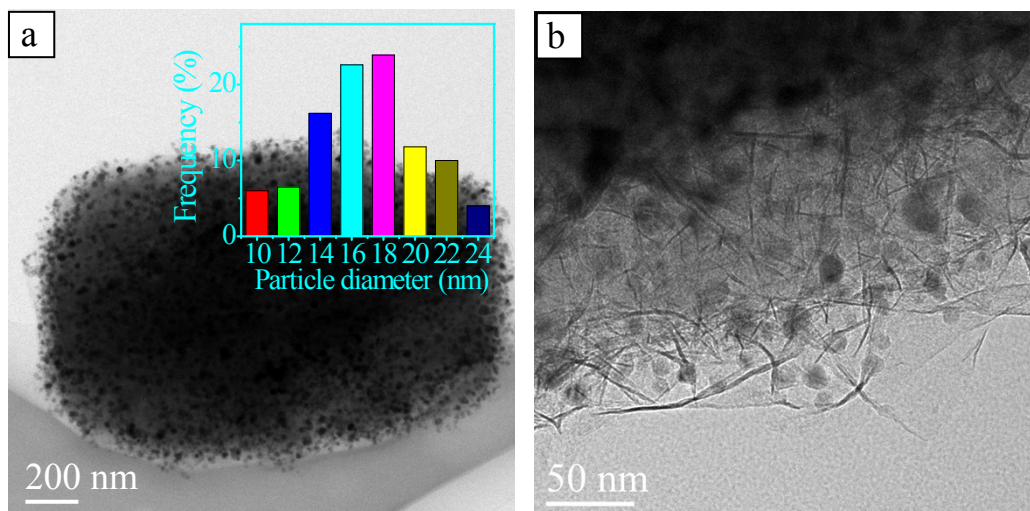


**Fig. S15** TEM images of ZSM-5@(Co/SiO<sub>2</sub>) after high-temperature treatment at 700 °C for 24 h in a flow of H<sub>2</sub>. The inset was the corresponding size distribution histogram of the Co nanoparticles.

*After treating at 700 °C for 24 h , the Co particle size of ZSM-5@(Co/SiO<sub>2</sub>) increased to 14 - 20 nm. The superior stability of ZSM-5@(Co/SiO<sub>2</sub>) was mainly because of the confining effect of the mesoporous SiO<sub>2</sub> matrices, which led to anti-sintering during high-temperature treatment.*

## References

1. D. Wang, L. Xu and P. Wu, *J. Mater. Chem., A*, 2014, **2**, 15535.
2. S. T. Gentry, S. F. Kendra and M. W. Bezpalko, *J. Phys. Chem., C*, 2011, **115**, 12736.
3. D. Santi, S. Rabl, V. Calemma, M. Dyballa, M. Hunger and J. Weitkamp, *ChemCatChem*, 2013, **5**, 1524
4. E. P. Parry, *J. Catal.*, 1963, **2**, 371.
5. D. L. Hoang, H. Berndt, H. Miessner, E. Schreier, J. Volter, H. Lieske, *Appl. Catal., A*, 1994, **114**, 295.